Radiation Physics and Chemistry 106 (2015) 77–82

Contents lists available at ScienceDirect

Radiation Physics and Chemistry

journal homepage: www.elsevier.com/locate/radphyschem

Short Communication

The synthesis of gold nanoparticles by a citrate-radiolytical method

Nikolina Hanžić [a], Tanja Jurkin [a,*], Aleksandar Maksimović [b], Marijan Gotić [a,*]

[a] Division of Materials Chemistry, Ruđer Bošković Institute, Bijenička 54, HR-10002 Zagreb, Croatia
[b] Division of Materials Physics, Ruđer Bošković Institute, Bijenička 54, HR-10002 Zagreb, Croatia

HIGHLIGHTS

- Gold nanoparticles were synthesised by classical and citrate-radiolytical methods.
- The size of gold nanoparticles was controlled by different saturated gases.
- Radiolytically intensified citrate oxidation is advantageous for Au(III) reduction.
- A comparison of particle sizes between classical and radiolytical methods was made.

ARTICLE INFO

Article history:
Received 3 April 2014
Accepted 8 July 2014
Available online 17 July 2014

Keywords:
Gold
Nanoparticles
Citrate
Gamma-irradiation
Radiolytical synthesis
Colloid

ABSTRACT

The classical citrate method is based on the reduction of an Au(III) precursor with sodium citrate in an aqueous solution near the boiling point. In this work gold nanoparticles (GNPs) were synthesised *via* a citrate method using reduction by gamma-irradiation at room temperature. The Au(III)–citrate aqueous precursor solution was gamma-irradiated to doses of up to 30 kGy. The dose rate of gamma-irradiation was ~8 kGy h^{-1}. The GNP size was controlled by the adsorbed dose as well as by different saturated gases (air or nitrogen) present in precursor solutions. The results showed that gamma-irradiation produced smaller GNPs in the presence of precursor solutions saturated with nitrogen compared with the ones saturated with air. By increasing both the gold(III) and citrate concentrations in precursor solutions, stable and highly concentrated colloidal gold/citrate suspensions were synthesised using classical and citrate-radiolytical reduction methods. Gamma-irradiation thus produced well-dispersed and highly concentrated GNPs in an aqueous citrate solution in the presence of dissolved oxygen and without adding any reducing or stabilising agents. Radiolytically intensified citrate oxidation and decarboxylation to acetone and other products by dissolved oxygen was advantageous for Au(III) reduction and subsequent formation of gold nanoparticles. Since the completely same precursor solutions were used both in the classical and citrate-radiolytical reduction methods, a real comparison of GNP sizes between these two methods was given.

1. Introduction

A chemical reduction of the Au(III) aqueous solution by citrate ions, the so called Turkevich–Frens method or "the classical citrate reduction method", is one of the most widely used synthesis procedures for obtaining rather uniform gold nanoparticles (GNPs). The classical citrate method (Turkevich et al., 1951; Frens, 1973) is based on the reduction of an Au(III) precursor with sodium citrate in an aqueous solution near the boiling point (100 °C). This synthesis produces GNPs in the form of a stable aqueous solution (colloidal gold or gold sol), since the citrate ions act both as reducing and protective agents. Citrate synthesised GNPs have been frequently used in various applications, especially biomedical. For instance, the surface of citrate coated GNPs can be modified by a biocompatible polymer or by anti-epidermal growth factor receptors in order to prolong the circulation time of GNPs in the bloodstream and/or for active cancer cell targeting (Reuveni et al., 2011). Apart from applications, the citrate reduction synthesis is one of the best model systems to study the GNPs nucleation-growth mechanism. Moreover, the new synthesis routes significantly contribute to a better understanding of the Au(III) reduction and GNPs formation mechanisms. For instance, Ji et al. (2007) emphasised the importance of adjusting the pH of the Au(III)/citrate solution above 6.2 in order to obtain nearly monodisperse GNPs. In addition to acting as reducing and protective agents, the citrate ions have thus played the third important role as pH mediators that determine the final size and size distribution of the GNPs. Kimling et al. (2006) and Plech et al. (2008) observed

* Corresponding authors. Tel./fax: +385 1 4561 123.
E-mail addresses: tjurkin@irb.hr (T. Jurkin), gotic@irb.hr (M. Gotić).

http://dx.doi.org/10.1016/j.radphyschem.2014.07.006
0969-806X/

that GNPs could be obtained by the citrate method *via* UV or X-ray reduction at room temperature. It was found that smaller and larger GNPs coexisted in the solution during growth and that electrostatic stabilisation defined their final size and shape. Ojea-Jiménez et al. (2010) synthesised GNPs by citrate reduction in the presence of heavy water (D_2O). The presence of deuterium increased the reducing strength of citrate molecules and as a consequence faster reduction produced smaller sized GNPs. Mikhlin et al. (2011) proposed a new mechanism of GNP formation by citrate reduction on the analogy of the originally proposed mechanism for the crystallisation of proteins. They proposed the formation of domains ("dense droplets") enriched by gold and the formation of GNP-containing globules that prevent the uncontrolled growth of gold nanoparticles. In a recent paper Doyen et al. (2013) suggest that citrate forms aggregates with Au(I) and/or Au(0) atoms and behaves as a "molecular linker", helping thus in the formation of GNPs. In this work we show that γ-irradiation could produce well-dispersed GNPs in an aqueous citrate solution in the presence of dissolved oxygen at room temperature and without adding any reducing agent or stabiliser. The enhanced radiolytical degradation (oxidation/decarboxylation) of citrate by dissolved oxygen and catalysed by gold had an advantage effect in the formation of gold nanoparticles.

2. Materials and methods

In this work the GNPs were synthesised by γ-irradiation of a gold/citrate aqueous precursor solution commonly used in case of a classical citrate reduction method. The auric acid ($HAuCl_4 \cdot 3H_2O$, Aldrich), trisodium citrate ($Na_3C_6H_5O_7$, Kemika) and Millipore deionised water (18.2 MΩ cm) were used. Glassware used in the experiments was cleaned by freshly prepared aqua regia (conc. HCl/conc. HNO_3=3:1 by volume). The precursor solution was prepared as follows: 20.5 μL of 4 wt% $HAuCl_4 \cdot 3H_2O$ was added to 10 mL of water in a glass vial while stirring with magnetic stirrer, then 200 μL of 1% citrate solution was added and stirred for additional 15 min. The molar ratio of gold to citrate was 1:3.2, which corresponds to the GNP sizes of approximately 12 nm. The concentrated samples were prepared by increasing the gold and citrate concentrations by three and ten times, respectively, whereas the H_2O volume and cit/Au ratio were kept fixed. Such

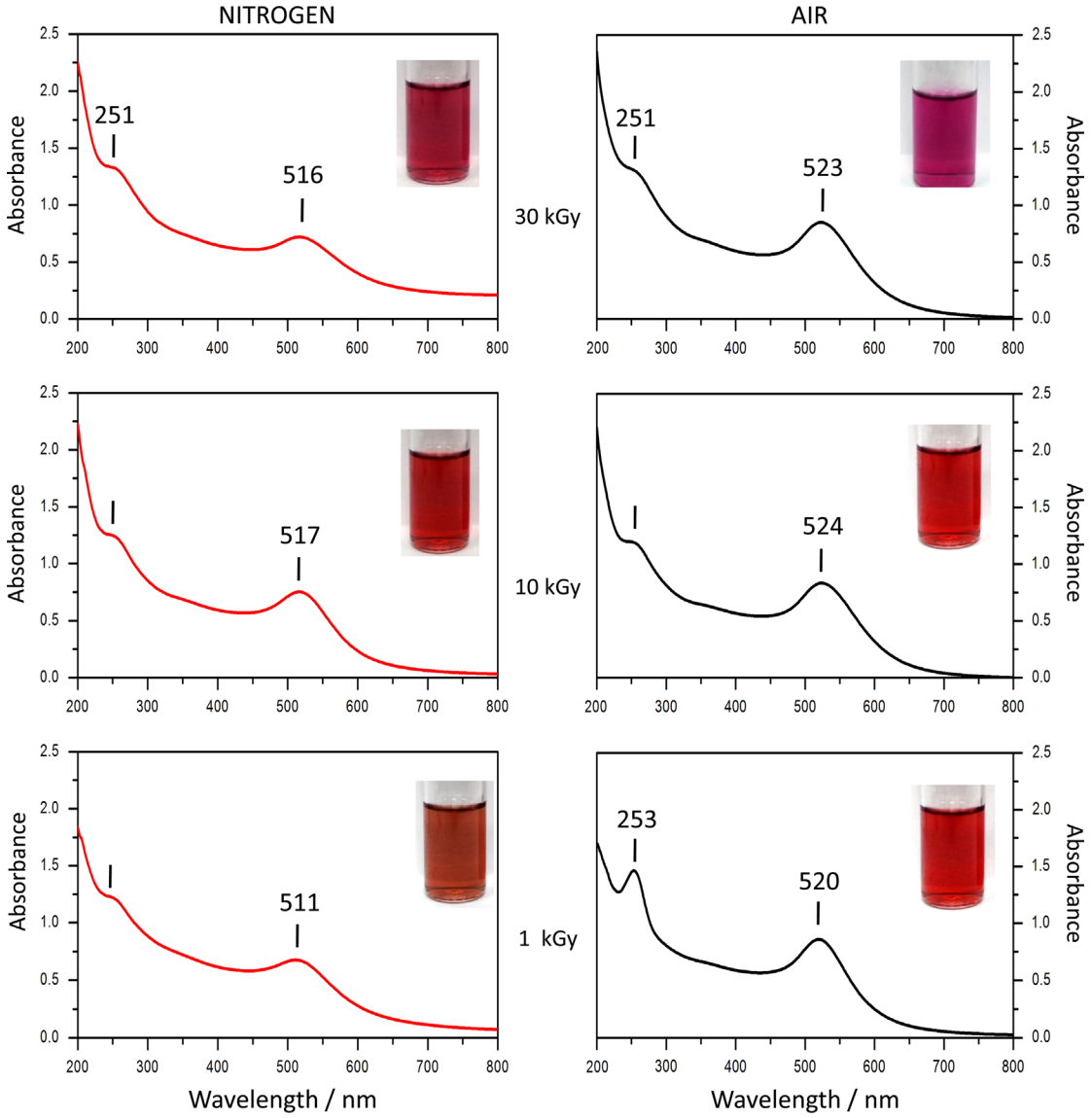

Fig. 1. UV–vis spectra of gold nanoparticle (GNP) samples synthesised by γ-irradiation of Au(III)/citrate solutions (absorbed doses of 1, 10 and 30 kGy). The left panel shows GNP samples synthesised in the presence of nitrogen gas (N_2), whereas the right one shows corresponding GNP samples synthesised by γ-irradiation in the presence of dissolved oxygen (air). Inset images show the colours of GNP samples.

prepared precursor solutions (containing dissolved oxygen) were γ-irradiated using a ^{60}Co source kept at the Division of Materials Chemistry of the Ruđer Bošković Institute. In the second series of experiments nitrogen gas (N_2) was bubbled into the precursor solutions prior to γ-irradiation. The dose rate of γ-radiation was ~8 kGy h^{-1} and the exact doses were 1, 10 and 30 kGy. The measured temperature of precursor solutions upon irradiation did not exceed 20 °C. The pH of precursor solutions was in the acidic range (between 5.3 and 5.7). A reference GNP sample was synthesised by the classical citrate method at 100 °C using the same precursor solution as in the case of γ-irradiation. The UV–vis spectra of colloidal gold samples were recorded using a UV/VIS/NIR spectrometer *Shimadzu* model UV-3600. The quartz cells having 1 cm optical path length were used. The size and shape of GNPs were evaluated using FE SEM model JSM-7000F manufactured by Jeol Ltd.

3. Results and discussion

Fig. 1 shows the UV–vis spectra of GNP samples synthesised by γ-irradiation of Au(III)–citrate precursor solutions at the doses of 1, 10 and 30 kGy, whereas Fig. S1 in Supplementary info shows the UV–vis spectrum of GNPs synthesised by the classical citrate reduction method at 100 °C. Generally, the position, width and intensity of surface plasmon resonance (SPR) band depend on GNP particle size, shape, concentration, surface charge, refractive index of the surrounding medium and interparticle interactions. The SPR bands for GNP samples synthesised by γ-irradiation in the presence of nitrogen were from 511 to 517 nm, whereas in the presence of air SPR bands were from 520 to 524 nm. The position of SPR bands has been regularly used for the determination of particle size. In this work we calculated particle size using the procedure presented by Haiss et al. (2007). The results of UV–vis and SEM characterisations of GNP samples are given in Table 1. The GNPs radiolytically synthesised at the dose of 10 kGy showed the narrowest size distribution.

The absorbance band at 253 nm (Fig. 1), fully developed and most prominent for the 1 kGy-air GNP sample and observable as a shoulder in all other samples deserves particular attention. However, it is difficult to assign this band without performing additional experiments. Fig. 2a shows the UV–vis spectra of 1 kGy-air GNP sample after ageing up to 25 days. The sample was kept in the fridge at 4 °C. The absorbance band at 253 nm gradually decreases with ageing and shifts from 253 nm to shoulder at 247 nm. The SPR band at 520 nm shows no changes in position, whereas its absorbance decreases from 0.86 to 0.81 (day 15), then again increases from 0.81 to 0.85 (day 25). The concentrated samples showed the same effect of ageing. In the subsequent experiments the sample was prepared a new and its UV–vis spectrum proved high reproducibility (Fig. 2b). Then the sample was centrifuged in order to completely separate GNPs from their colloidal solution. The UV–vis spectrum of thus obtained clear solution is shown in Fig. 2b (lower spectrum). The UV–vis band at 523 nm related to gold nanoparticles completely disappeared, whereas the fully developed band at 254 nm was still present.

The UV–vis spectrum of Au(III)/citrate precursor solution prior to irradiation has the absorbance bands at 216 and 285 nm, respectively, but does not contain a band at about 250 nm (Fig. S2 in Supplementary material). Citrate alone and the γ-irradiated citrate aqueous solution showed no UV–vis bands (results not shown). Fig. S3a shows the UV–vis spectrum of 1,3-acetonedicarboxylic acid (dicarboxyacetone-DCA) aqueous solution. DCA absorbed UV and showed two bands at 297 and 242 nm. These two UV bands converted to the band at 238 nm in the colloidal gold sample obtained by reduction with DCA at room temperature. The new band at 238 nm could be assigned to oxidation/decarboxylation products of DCA. Dicarboxyacetone is the oxidation product of citrate ions and plays an important role in the classical citrate reduction method acting as a reducing, complexing and nucleating agent. DCA is a stronger reducing agent than citrate ions, hence able to produce gold nanoparticles at room temperature. However, when the DCA concentration reaches maximum it decomposes (oxidises) to acetone, acetoacetate and formate ions and/or other products (Kumar et al., 2007; Doyen et al., 2013). DCA decomposition is catalysed by the gold nanoparticle surface. Fig. S3b shows the UV–vis spectrum of gold colloidal solution (lower spectrum) and the same gold colloidal solution where the small amount of acetone was added (upper spectrum). The new UV band and 260 nm due to the added acetone is very similar to the UV

Table 1
UV–vis and SEM characterisation of GNP synthesised samples; comparison between gold particle sizes obtained by classical and citrate-radiolytical methods.

Samples	$c(HAuCl_4)$ (mol dm^{-3})	λ_{SPR} (nm)	A_{SPR}	A_{450}	Gold nanoparticle size (nm)			Gold nanoparticle concentration (mol dm^{-3})	
					UV–vis[a]	SEM[b]		UV–vis[a]	SEM[c]
						mean	sigma		
Classic	2.0×10^{-4}	519	1.00	0.60	18.0	11.2	0.21	1.5×10^{-9}	4.7×10^{-9}
Classic (3 ×)	6.0×10^{-4} (3 ×)	518	2.38	1.45	16.0	10.9	0.27	5.4×10^{-9}	1.5×10^{-8}
Classic (10 ×)	2.0×10^{-3} (10 ×)	522	6.96[d]	4.12[d]	18.0	14.1	0.26	1.1×10^{-8}	2.4×10^{-8}
1 kGy, N_2	2.0×10^{-4}	511	0.67	0.58	3.5	–	–	1.6×10^{-7}	–
10 kGy, N_2	2.0×10^{-4}	517	0.75	0.57	6.0	–	–	4.5×10^{-8}	–
30 kGy, N_2	2.0×10^{-4}	516	0.72	0.61	4.0	–	–	1.7×10^{-7}	–
1 kGy, Air	2.0×10^{-4}	520	0.86	0.57	10.0	11.2	0.25	9.3×10^{-9}	4.7×10^{-9}
10 kGy, Air	2.0×10^{-4}	524	0.83	0.55	11.0	11.0	0.19	6.6×10^{-9}	4.9×10^{-9}
30 kGy, Air	2.0×10^{-4}	523	0.85	0.57	10.0	11.1	0.21	9.2×10^{-9}	4.8×10^{-9}
10 kGy, Air (3 ×)	6.0×10^{-4} (3 ×)	526	2.08	1.26	16.0	12.1	0.18	4.7×10^{-9}	1.1×10^{-8}
10 kGy, Air (10 ×)	2.0×10^{-3} (10 ×)	524	4.80[d]	2.96[d]	14.0	11.6	0.20	1.7×10^{-8}	4.2×10^{-8}
30 kGy, Air (3 ×)	6.0×10^{-4} (3 ×)	524	2.68	1.62	16.0	12.4	0.18	6.1×10^{-9}	1.0×10^{-8}
30 kGy, Air (10 ×)	2.0×10^{-3} (10 ×)	517	–	–	–	–	–	–	–

[a] UV–vis determining gold nanoparticle size and concentration using the procedure presented by Haiss et al. (2007). The method is based on the relative A_{SPR}/A_{450} ratio, which is the reason why both values are given in this table.

[b] Particle diameters were measured using the ImageJ software from SEM images, whereas particle size distribution was calculated using the LogNormal function. The parameter sigma in the LogNormal function is related to the distribution width, therefore a smaller sigma represents narrower particle size distribution.

[c] SEM determining GNP concentration calculated using the equation (Liu et al., 2007); $c_{GNPs}=c(HAuCl_4)/30.9-D^3$, where c_{GNPs} is the concentration of gold nanoparticles (mol dm^{-3}), $c(HAuCl_4)$ is the concentration of gold salt (mol dm^{-3}) and D is the measured diameter of the GNPs (nm).

[d] Obtained by multiplying the observed absorbance by its dilution factor (50% dilution).

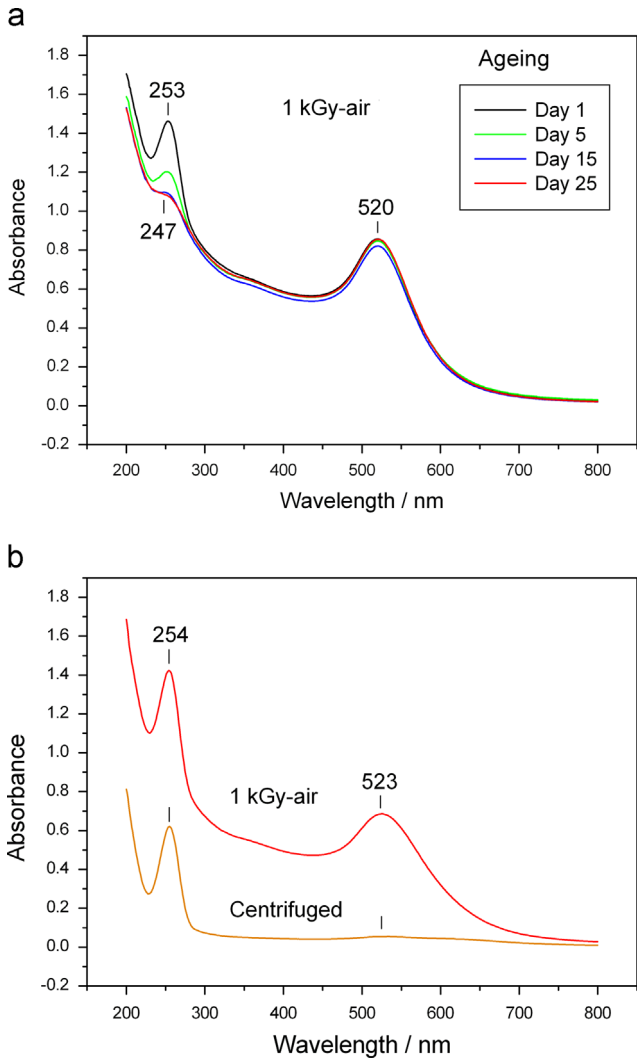

Fig. 2. (a) The UV–vis spectra of 1 kGy-air sample after ageing up to 25 days. The absorbance band at 253 nm gradually decreases with ageing and shifts from 253 to 247 nm. The SPR band at 520 nm shows no changes in position, whereas its absorbance decreases from 0.86 to 0.81 (day 15), then again increases to 0.85 nm (day 25). (b) The UV–vis spectrum of newly prepared 1 kGy-air sample and the UV–vis spectrum of a clear solution obtained upon centrifugation of the colloidal gold solution.

band at 253 nm in sample 1 kGy-air. The difference in position of the band could arise from physically added acetone, whereas in the sample acetone is radiolytically formed by decomposition of citrate and/or dicarboxyacetone. Thus, in the present work it seems reasonable to infer that an enhanced degradation (oxidation) of citrate and DCA to acetone was achieved by the synergistic effect of radiolytical oxidation in the presence of dissolved oxygen and gold nanoparticle surface. The UV–vis band at 253 nm is assigned to the acetone (the presence of the small amount of other decarboxylated products is not excluded), which was an intermediate products obtained by radiolytically enhanced degradation of citrate and dicarboxyacetone. Acetone was stable up to 15 days when the sample was kept in the fridge at 4 °C, however the UV band at 253 disappeared after one day when the sample was kept at room temperature (result not shown).

Fig. 3 shows SEM images and the corresponding particle size distribution of GNP samples synthesised by γ-irradiation in the presence of dissolved oxygen (air). The SEM images of GNP samples radiolytically synthesised in the presence of dissolved nitrogen are shown in Fig. S3 (Supplementary material). The GNP

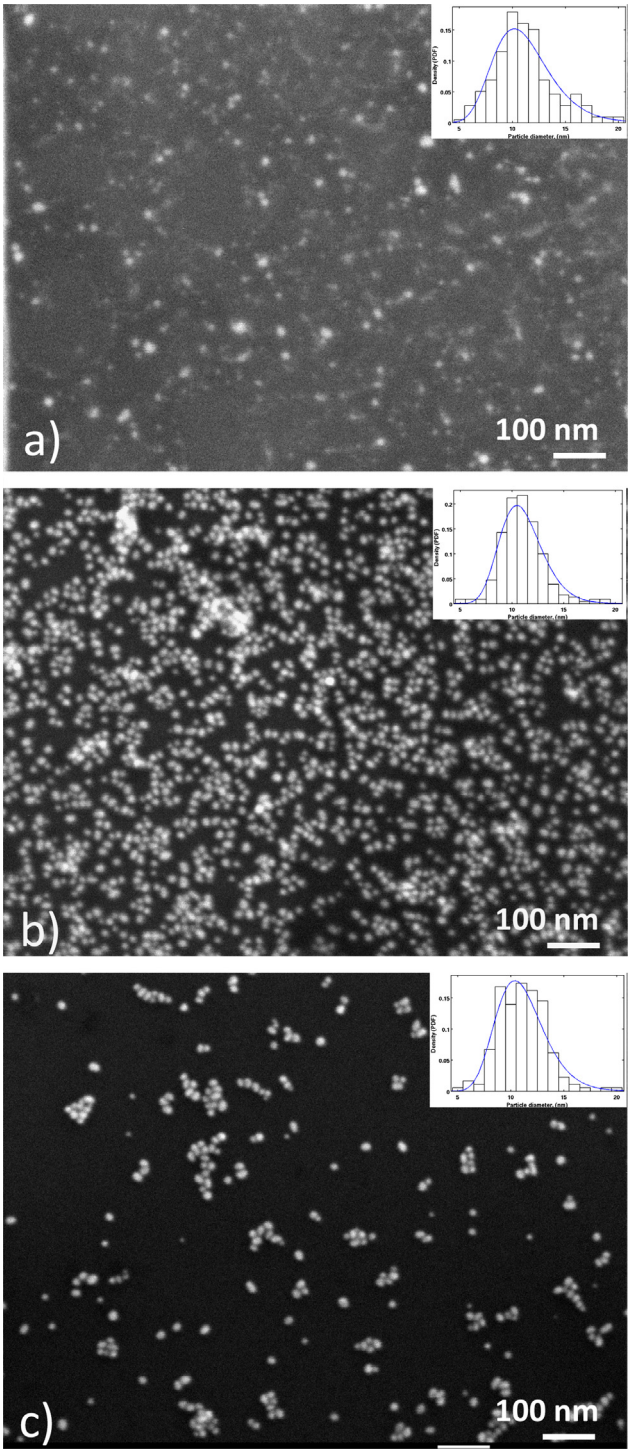

Fig. 3. FE SEM images of GNP samples synthesised by γ-irradiation of Au(III)/citrate solution in the presence of air at 1 kGy (a), 10 kGy (b) and 30 kGy (c). Inset images show the corresponding particle size distribution.

sizes measured by SEM and the GNP size estimations by UV–vis are compared in Table 1.

Fig. 4 shows the UV–vis spectra of two GNP samples synthesised by γ-irradiation of highly concentrated Au(III)/citrate solutions at a dose of 10 kGy in the presence of dissolved oxygen. The 10 × concentrated sample was recorded after 50% dilution (asterisk). Generally, the SPR absorbance maximum is related to GNP concentration. The GNP concentrations calculated on the basis of UV–vis absorbance are given in Table 1. The most concentrated sample investigated in this work has the SPR band at 524 nm with an

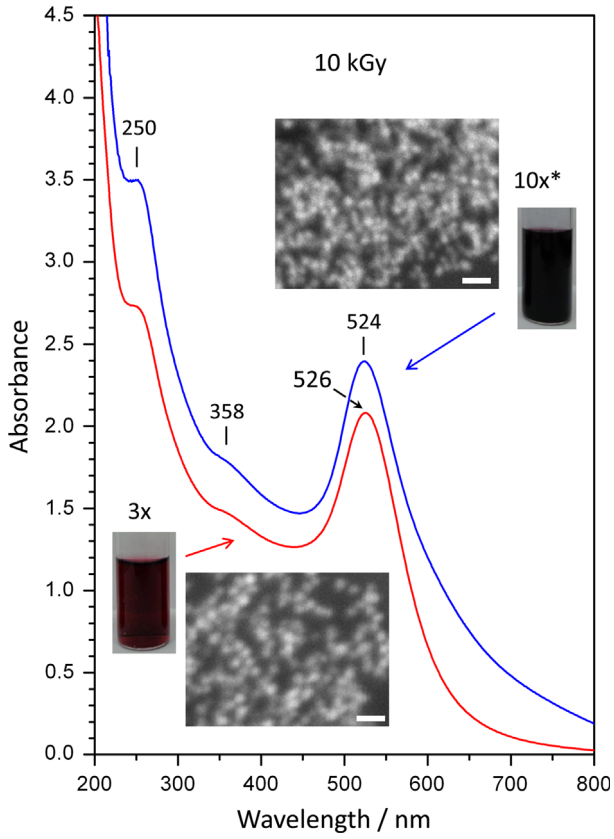

Fig. 4. UV–vis spectra of GNP samples synthesised by γ-irradiation of highly concentrated Au(III)/citrate precursor solutions at the absorbed dose of 10 kGy in the presence of air; the upper spectrum – 10 times higher gold concentration recorded after 50% dilution (asterisk) and the lower spectrum – 3 times higher gold concentration in comparison with a classic citrate sample. Inset images show the corresponding SEM images; the scale bars are 50 nm.

absorbance maximum of 4.8 (obtained by multiplying the observed absorbance by its dilution factor), which can be regarded as a highly concentrated colloidal gold aqueous suspension obtained at room temperature.

The nanoparticle radiolytical synthesis from aqueous solutions as a rule includes the use of radical scavengers (such as 2-propanol for scavenging hydroxyl radicals ($HO^{\bullet}$), which are very strong oxidative species)) and various colloidal stabilisers such as PVP (poly(vinylpyrrolidone)), PEG (polyethylene glycol), etc. (Li et al., 2007). The precursor solution should be purged with nitrogen gas in order to prevent the conversion of highly reactive reducing radicals, *i.e.*, hydrated electrons (e_{aq}^{-}) and $H^{\bullet}$ with dissolved oxygen, to corresponding $O_2^{\bullet -}$ and $HO_2^{\bullet}$ radicals which possess oxidising abilities (Makarov et al., 2014). However, in this work the GNPs were prepared by the citrate-radiolytical method using neither scavengers nor stabilisers. Besides, the citrate-radiolytical reduction took place in the presence of dissolved oxygen (air). The GNPs synthesised in the presence of air were approximately two times larger than the GNPs synthesised in the presence of nitrogen. This is because the final size of gold nanoparticles markedly depends on the reducing conditions.

At highly reducing conditions, as in the case of γ-irradiation of nitrogen saturated solutions and at a relatively high dose rate (~ 8 kGy h^{-1}) the hydrated electrons (e_{aq}^{-}) are provided to the gold solutions fast enough, to the effect that Au(III) and Au(I) rapidly reduce to isolated Au(0) atoms (Dey et al., 2011), thus providing for a high nucleation rate and coalescence of the gold nuclei into small final-sized gold nanoparticles (Polte et al., 2010).

On the contrary, in the air saturated solutions there is a competition between reducing (e_{aq}^{-} and organic radicals) and oxidising species ($O_2^{\bullet -}$ and $HO_2^{\bullet}$ radicals) and the Au(III) ions are only partially reduced, because the amount of a strong reducing species is insufficient to completely reduce the Au(III) and Au(I) to Au(0). Weak reducing agents such as citrate ions have too positive reduction potential to be able to reduce free Au(I) ions in a solution to isolated Au(0) atoms. However, as soon as solid gold clusters formed the Au(I) ions adsorbed on them. The Au(I) ions adsorbed on gold clusters are easily reduced by weak reducing agents, because the redox potential of gold ions adsorbed on the same metal clusters is more positive than the one of free ions in solutions (Gachard et al., 1998; Abidi and Remita, 2010). Hence at a slower reduction rate such as the radiolytic reduction in air saturated solutions bigger sized (~11 nm, Table 1) gold nanoparticles were formed. Moreover, the difference in reduction conditions between the air and nitrogen saturated Au(III)/citrate solutions is most visible on the UV–vis spectra recorded for samples obtained at a dose up to 1 kGy (Fig. 1), which corresponds to the reaction time of 7.5 min (actually the red gold sol appeared even at a dose of 0.5 kGy, results not shown).

On the other hand, an easy radiolytical reduction of the Au(III)/citrate precursor solution in the presence of dissolved oxygen suggests that citrate ions are good scavengers for oxidative radicals and that the citrate and Au(III) are in close proximity, enabling thus an easy electron transfer from citrate to Au(III) ions. This is in line with the work of Mikhlin et al. (2011) who suggested that the Au(III)/citrate aqueous solution system resembled a microemulsion with "droplets" and globules confining the GNP growth. It is known that an easy mass exchange and transfer of electrons from a reducing to an oxidising agent is possible in γ-irradiated microemulsions, favouring thus the reduction processes (Gotić et al., 2007, 2009).

4. Conclusion

The γ-irradiation of Au(III)/citrate precursor solutions produced well-dispersed and highly concentrated gold colloids in the presence of dissolved oxygen, without adding any reducing or protective agents. GNP particle size can be controlled by choosing the saturated gases (air or nitrogen) present in the precursor solution. The GNPs synthesised in the presence of air ($\approx$ 10 nm) were approximately two times larger than the GNPs synthesised in the presence of nitrogen ($\approx$ 5 nm), as determined by UV–vis spectroscopy. An easy radiolytical reduction of the Au(III)/citrate precursor solution in the presence of dissolved oxygen could be explained by enhanced radiolytical oxidation/decarboxylation of citrate to dicarboxyacetone, acetone and other products. Thus, the radiolytical degradation of citrate produced stronger reducing agents than citrate ions themselves. A real comparison of GNP sizes between the classical citrate and citrate-radiolytical reduction methods was possible, because in this work the identical precursor solutions were used in both synthesis routes.

Acknowledgments

The authors wish to thank Mr Milan Blažević and Dr Branka Mihaljević for the technical assistance on gamma-irradiation and Dr Jacqueline Belloni for the helpful discussion regarding the radiolytic reduction of Au(III) ions.

Appendix A. Supplementary material

Supplementary data associated with this article can be found in the online version at http://dx.doi.org/10.1016/j.radphyschem.2014.07.006.

References

Abidi, W., Remita, H., 2010. Gold based nanoparticles generated by radiolytic and photolytic methods. Rec. Paten Eng. 4, 170–188.

Dey, G.R., El Omar, A.K., Jacob, J.A., Mostafavi, M., Belloni, J., 2011. Mechanism of trivalent gold reduction and reactivity of transient divalent and monovalent gold ions studied by gamma and pulse radiolysis. J. Phys. Chem. A 115, 383–391.

Doyen, M., Bartik, K., Bruylants, G., 2013. UV–Vis and NMR study of the formation of gold nanoparticles by citrate reduction: observation of gold–citrate aggregates. J. Colloid Interface Sci. 399, 1–5.

Frens, G., 1973. Controlled nucleation for the regulation of the particle size in monodisperse gold suspensions. Nat. Phys. Sci. 241, 20–22.

Gachard, E., Remita, H., Khatouri, J., Keita, B., Nadjo, L., Belloni, E., 1998. Radiation-induced and chemical formation of gold clusters. New J. Chem., 1257–1265.

Gotić, M., Jurkin, T., Musić, S., 2007. Factors that may influence the micro-emulsion synthesis of nanosize magnetite particles. Colloid Polym. Sci. 285, 793–800.

Gotić, M., Jurkin, T., Musić, S., 2009. From iron(III) precursor to magnetite and vice versa. Mater. Res. Bull. 44, 2014–2021.

Haiss, W., Thanh, N.T.K., Aveyard, J., Ferning, D.G., 2007. Determination of size and concentration of gold nanoparticles from UV–vis spectra. Anal. Chem. 79, 4215–4221.

Ji, X., Song, X., Li, J., Bai, Y., Yang, W., Peng, X., 2007. Size control of gold nanocrystals in citrate reduction: the third role of citrate. J. Am. Chem. Soc. 129, 13939–13948.

Kimling, J., Maier, M., Okenve, B., Kotaidis, V., Ballot, H., Plech, A., 2006. Turkevich method for gold nanoparticle synthesis revisited. J. Phys. Chem. B 110, 15700–15707.

Kumar, S., Gandhi, K.S., Kumar, R., 2007. Modeling of formation of gold nanoparticles by citrate method. Ind. Eng. Chem. Res. 46, 3128–3136.

Li, T., Park, H.G., Choi, S.-H., 2007. γ-Irradiation-induced preparation of Ag and Au nanoparticles and their characterizations. Mater. Chem. Phys. 105, 325–330.

Liu, X., Atwater, M., Wang, J., Huo, Q., 2007. Extinction coefficient of gold nanoparticles with different sizes and different capping ligands. Colloids Surf., B 58, 3–7.

Makarov, I.E., Metreveli, P.K., Metreveli, A.K., Ponomarev, A.V., 2014. The effect of electron irradiation on aqueous dispersion of humic acids and lignin. Radiat. Phys. Chem. 97, 12–15.

Mikhlin, Y., Karacharov, A., Likhatski, M., Podlipskaya, T., Zubavichus, Y., Veligzhanin, A., Zaikovski, V., 2011. Submicrometer intermediates in the citrate synthesis of gold nanoparticles: new insights into the nucleation and crystal growth mechanisms. J. Colloid Interface Sci. 362, 330–336.

Ojea-Jiménez, I., Romero, F.M., Bastús, N.G., Puntes, V., 2010. Small gold nanoparticles synthesized with sodium citrate and heavy water: insights into the reaction mechanism. J. Phys. Chem. C 114, 1800–1804.

Plech, A., Kotaidis, V., Siems, A., Sztucki, M., 2008. Kinetics of the X-ray induced gold nanoparticle synthesis. Phys. Chem. Chem. Phys. 10, 3888–3894.

Polte, J., Ahner, T.T., Delissen, F., Sokolov, S., Emmerling, F., Thünemann, A.F., Kraehnert, R., 2010. Mechanism of gold nanoparticle formation in the classic citrate synthesis method derived from coupled in situ XANES and SAXS evaluation. J. Am. Chem. Soc. 132, 1296–1301.

Reuveni, T., Motiei, M., Romman, Z., Popovtzer, A., Popovtzer, R., 2011. Targeted gold nanoparticles enable molecular CT imaging of cancer: an in vivo study. Int. J. Nanomed. 6, 2859–2864.

Turkevich, J., Stevenson, P.C., Hillier, J., 1951. A study of the nucleation and growth processes in the synthesis of colloidal gold. Discuss. Faraday Soc 11, 55–75.